Performance Characterization of the Hyperion Imaging Spectrometer Instrument

Lushalan Liao, Peter Jarecke, Darrel Gleichauf and Ted Hedman

TRW Space and Electronics Group
Electro-Optical Systems and Technology Department

ABSTRACT

This paper presents the techniques and results of Hyperion laboratory characterization. Hyperion is a hyperspectral imager scheduled to fly on the Earth-Orbiter 1 (EO-1) spacecraft for the New Millennium project. The other payloads on the spacecraft are ALI (Advanced Land Imager) and AC (atmospheric corrector). The payloads were integrated into the spacecraft at Goddard Space Flight Center (GSFC). An End-to-End imaging test was conducted at GSFC which demonstrated integrity of Hyperion performance after environmental tests. The performance characterization procedures described here include: crosstrack MTF, spectral and spatial co-alignment, spectral wavelength calibration, signal to noise, polarization, spectral response function and scene generation. The characterization was carried out with the TRW Imaging Spectrometer Characterization Facility which is based on a 250 watt QTH lamp, a monochromator, a collimator and a fine pointing mirror. A selection of narrow slits and a knife edge are illuminated at the exit slit of the monochromator for sub-pixel performance characterization parameters such as MTF. Special attention is devoted to the spectral calibration technique using rare earth doped Spectralon panels. This was the technique used at the End-to-End test to verify spectral performance of Hyperion after GSFC environmental tests. It is a particular useful technique when the optical test setup does not allow for the use of a monochromator.

1. Introduction

The New Millennium Program (NMP) is an initiative to demonstrate advanced technologies and designs that show promise for dramatically reducing the cost and improving the quality of instruments and spacecraft for future space missions. Under this program, missions are intended primarily to validate such technologies and designs in flight by providing useful science data to the user community. The goal is to make future operational spacecraft "faster, cheaper and better", through incorporation of the technologies validated in the NMP. The Earth Orbiter missions will validate by space flight, advanced technologies for the next generation Earth Science Systems Program Office science needs.

The EO-1 spacecraft will be launched on a Delta II Med-Lite 7320-10 launch vehicle. The EO-1 will have a sun-synchronous orbit with an altitude of 705 km and a 10:01 AM descending node. The orbit inclination is 98.2 degree, the orbital period is 98.9 minutes, and the EO-1 equatorial crossing time is one minute behind Landsat-7. The velocity of the EO-1 nadir point is 6.74 km/sec. The EO-1 satellite will fly in formation with the Landsat 7 satellite in a sun-synchronous, 705 km orbit with a 10:01 am descending node. That is, it will be in an orbit that covers the same ground track as Landsat 7, approximately one minute later. The objective is to obtain images of the same ground areas at nearly the same time, so that they may be directly compared. There are three primary instruments on the first Earth Orbiter satellite (EO-1) under the NMP of the National Aeronautics and Space Administration (NASA): the Advanced Land Imager (ALI), the Hyperion and the LEISA Atmospheric Corrector (LAC). The EO-1 satellite is co-manifested with Argentina's SAC-C (Scientific Applications Satellite) and is scheduled for launch from the Western Test Range on a Delta 7320 in the later part of 2000.

The Hyperion instrument operates in a push-broom fashion with two spectrometers, one operating at visible and near infrared wavelengths (VNIR) and one at short-wave infrared (SWIR) wavelengths. The spectrometers share a single set of fore-optics and a common slit that defines the along-track (the short dimension of the slit) and cross-track (the long dimension of the slit) dimensions. The dispersion of the scene radiation, as defined by the slit, is achieved by a grating in each spectrometer. Radiation from the slit is split into two beams for each spectrometer using a beamsplitter. Each path is focused onto a row of focal plane array (FPA) pixels (the spatial dimension of the FPA) and the grating disperse the scene spectra onto the other dimension (the spectral dimension) of the 2-dimensional FPA. As the spacecraft flies over the scene, an image is formed with the spatial pixels imaging the scene in a push-broom manner. A hyperspectral "image cube" of the scene is formed by the image data from the various spectral pixels. The Hyperion instrument consists of 3 physical units (Figure 3.1-1), (1) the Hyperion Sensor Assembly (HSA), (2) the Hyperion Electronics Assembly (HEA), and (3) the Cryocooler Electronics Assembly (CEA). A layout of the Hyperion instrument is shown in Figure 1. A performance summary of the Hyperion sensor is given in Table 1.

This paper describes the processes for radiometric characterization of the Hyperion sensor for the following parameters: crosstrack MTF, spectral and spatial co-alignment, spectral wavelength calibration, spectrometer slit profile, and signal to noise. The characterization of the Hyperion Imaging Spectrometer Instrument builds on the experience of two previous instrument tests programs at TRW. They are the Lewis Hyperspectral Imager for the NASA Small satellite Technology Initiative Program (Ref 1) and the TRWIS 3 Imaging Spectrometer (Ref 2 and Ref 3). The TRW Imaging Spectrometer Characterization Facility is used for performance characterization Ref (4). Additional capital upgrades were made to the facility for Hyperion characterization.

The calibration process for sensor spectral responsivity was changed and a new secondary standard, the Spectralon Panel Assembly (SPA), was created and made traceable to three primary standards: two high quantum efficiency Si trap detectors and an electrically calibrated pyroelectric radiometer. The SPA utilizes an FEL Sylvania 1000 watt lamp and a panel of Spectralon. The primary standard validation and radiance scale realization and the secondary standard design and validation are described in an accompanying paper titled, "Radiometric Calibration of the Hyperion Imaging Spectrometer Instrument From Primary Standards to End-to-End Calibration. "

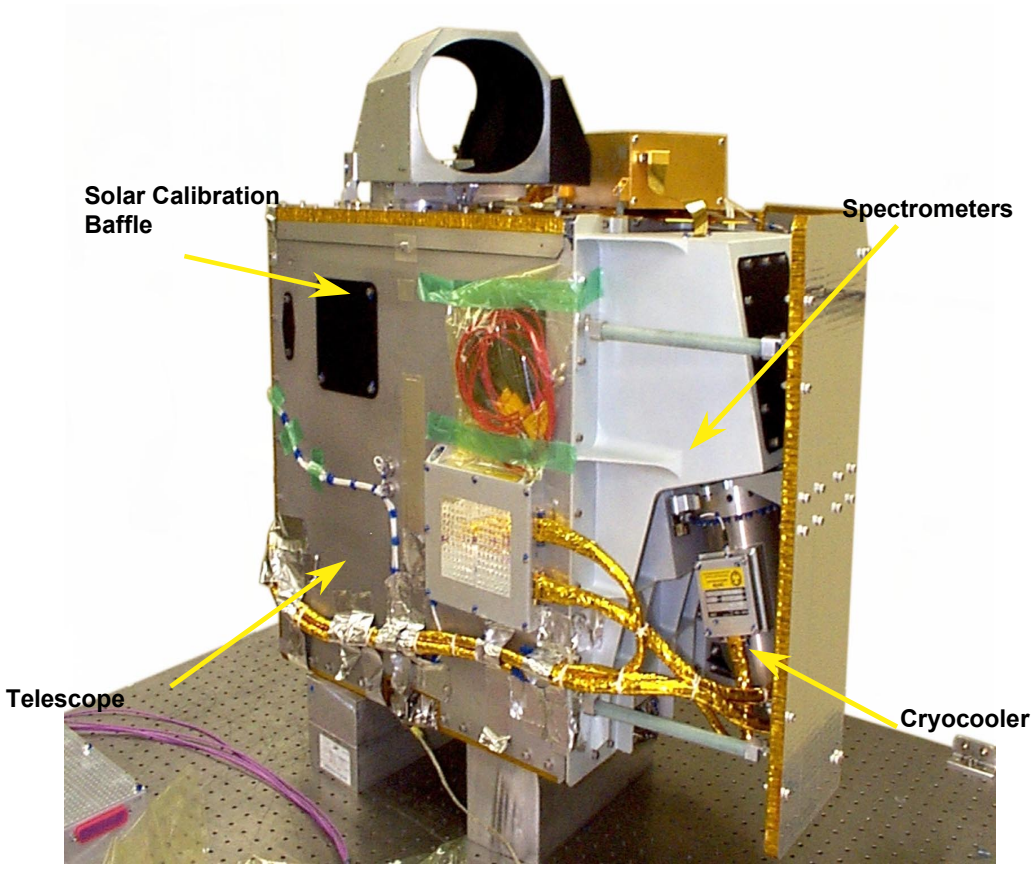

Figure 1 The Hyperion Instrument Layout

Instrument Parameter	Hyperion Instrument Characteristic
GSD at 705 km Altitude	30 m
Swath Width (km)	7.5 km
Spectral Coverage	0.4 - 2.5 μm
Imaging Aperture	12.5 cm diameter
On-orbit Life	1 year (2 years goal)
Instantaneous Field of View	42.5 μrad
Number of Spectral Channels	220
Spectral Bandwidth	10 nm
Cross-track Spectral Error	<1.5 nm (VNIR), <2.5 nm (SWIR) (TBR)
Spatial Co-registration of Spectral Bands	<20% of Pixel (TBR)
Absolute Radiometric Accuracy	<6% (1 sigma)
Data Quantization	12-bit
Instrument Weight	49 kg
Instrument Power Consumption	78 Watts Orbit Average

Table 1 Hyperion Instrument Characteristics

2. Radiometric Performance Characterization

2.1. TRW Imaging Spectrometer Characterization Facility

A layout of the TRW Imaging Spectrometer Characterization Facility, previously referred to as the Multi-Spectral Test Bed (MSTB) is shown in Figure 2. There are two modes of operation. Both are shown simultaneous in Figure 2. In one, the end of a light pipe (which is fed by the output of a monochromator) illuminates a knife edge or a pinhole. This pinhole is at the focus of a 0.25 meter diameter off-axis parabola (OAP) which collimates the beam and directs it to a 0.3 meter diameter flat mirror. This is done by the small fold mirror shown just below the pinhole. The focus condition of the pinhole is established separately with an interferometer. The flat fine pointing mirror sits on a precision 2-axis mount with a step size of 10 microradians. The beam from this fold mirror is directed through the vacuum chamber window to the entrance aperture the sensor under test. The AΩ of the characterization facility is such that the aperture and field of view of Hyperion is fully flooded. The two stage fine pointing fold mirror can cause the knife edge or pinhole to move in discrete steps across any pixel in the cross-track or spectral direction.

In the second mode of use of the Spectrometer Facility, the end of the light pipe is re-imaged onto a Spectralon panel, which is at the focus of the off-axis collimator by removal of the small fold mirror. The primary use of this mode is for spectral wavelength calibration of the focal plane array. This is described in 2.3, a Spectralon panel doped with a rare earth (holmium oxide and erbium oxide are both used) is imaged and ratioed to the image from the highly reflecting panel. The spectral reflectance of the doped materials are well known and stable.

Also shown in Figure 2, is a secondary transfer standard radiometer that provides absolute calibration of the radiance in the beam from the Spectrometer Facility. It is removed so that the fine pointing mirror beam can enter the vacuum chamber window to illuminate the sensor. The transfer radiometer has a chopped pyroelectric detector, which has been made traceable to the primary irradiance scale mentioned above. The transfer radiometer has a precision AΩ that has been calculated from component data.

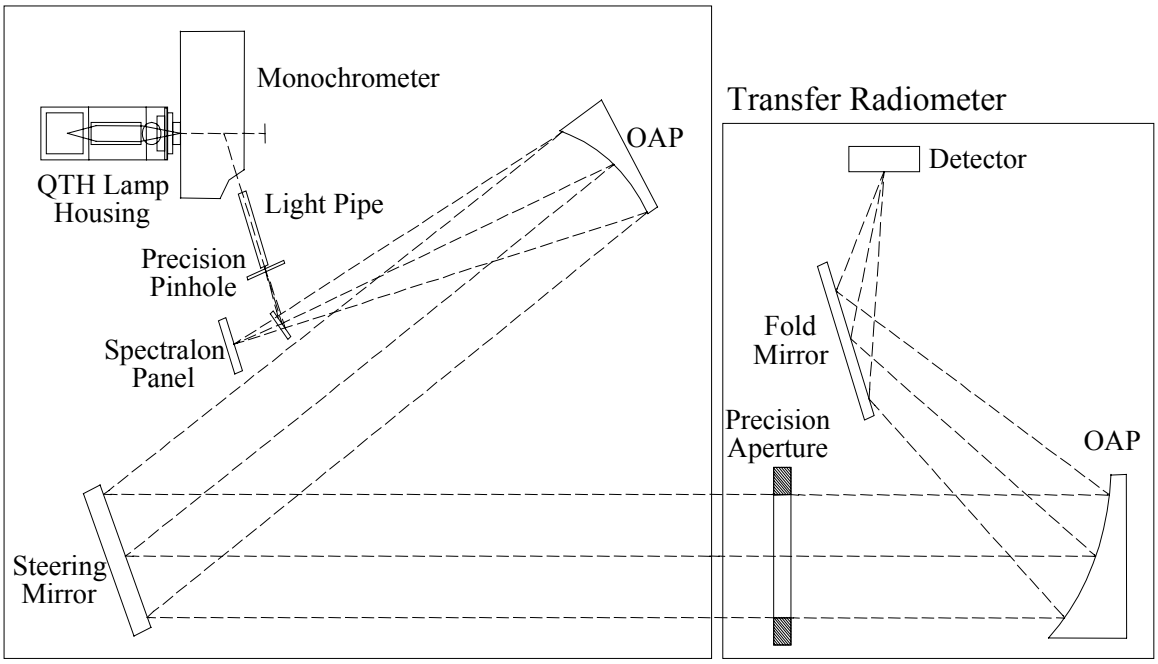

Figure 2 The TRW Imaging Spectrometer Characterization Facility is Shown in the Left Box With the off-axis parabola (OAP) Collimator Focus at the Object Plane at the End of the Light Pipe. Light From the Monochromator is Focussed onto the Entrance to the Light Pipe. The Box on the Right is the Transfer Radiometer for Calibrating the Output of the Spectrometer Facility

2.2. Alignment and Image Quality

2.2.1. Spectral and Spatial Alignment

The purpose of the spectral and spatial alignment is to measure the extent to which the curves of constant field-of-view (isofov) and constant wavelength (isolamda) deviate from the rectilinear grid defined by the phsyical pixels of the focal plane array (FPA). During the assembly of Hyperion, the FPA is rotated so that the isofov and isolamda curves line up as well as possible with the two rectilinear dimension of the FPA. The residual error not removed by the rotation, or induced by latter environmental testing is the misalignment in the sepctral and spatial dimension.

Cross-track spectral alignment (CTSA) is a measure of how much an isolamda curve deviates from the spectral dimension of the FPA. To measure CTSA error, the monochromator is set to a wavelength with a slit width that narrow in wavelength relative to spectral resolution of a pixel so that the line shape mapped out has minimal effect from the light source. Then, the monochromator is stepped in fractional pixel steps of wavelength to determine the center wavelength for a pixel located at a particular FOV position. Examples of spectral profile produced by this measurement are shown in Figure 6. Five FOV positions were chosen across the total FOV for characterization. An example of the plot of the center wavelengths of a given spectral channel across the FOV positions is shown in Figure 3. The maximum deviation of this curve from a constant is the measure of CTSA error. As can be seen from Figure 3, the peak to peak difference for SWIR channel 126 is less than 1 nm, well within the specification. On the other hand, the peak to peak VNIR CTSA error is about 2.7 nm, exceeding the specification allocated error.

Spatial co-registration of spectral channels (SCSC) is a measure of how much an isofov curve deviates from the the spatial dimension of of the FPA. For this measurement, we installed a narrow slit target, perpendicular to the entrance slit of the instrument, at the image plane of the Spectrometer Facility. The purpose of the narrow slit target is to limit the illumination to only 1 pixel in the cross-track direction. We then illuminate this narrow slit target with a broadband light source by placing the monochromator in the zeroth mode. The Hyperion instrument spectrometer

will then disperse the broadband light into the various spectral channels. The variation in the location of the peak of the signal as a function of the spectral channel is then the measure of the spatial co-registration of the spectral channels. Figure 4 shows a plot (left hand side of the figure) of the deviation from perfect alignment at 20 locations along the FOV. It shows Hyperion results that exceed the specification in the SWIR while meeting VNIR specification.

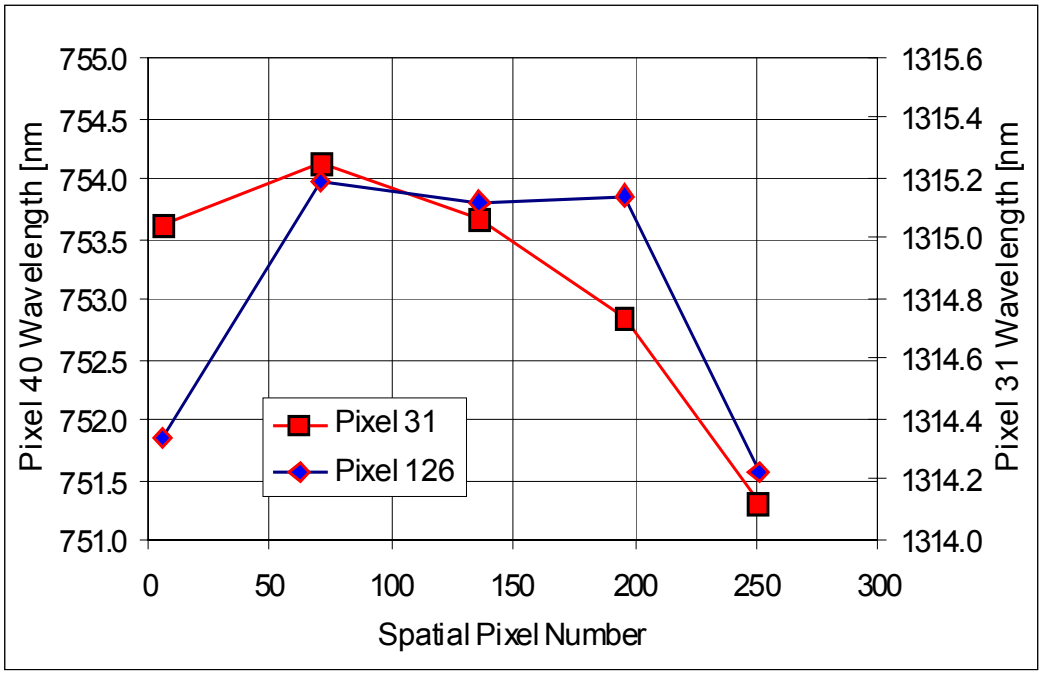

Figure 3 Example CTSA error for VNIR (channel 31) and SWIR (channel 126)

2.2.2. Image Quality

During the assembly of Hyperion, the best focus of the Hyperion sensor is achieved by inserting shims under the FPA assembly. The best focus location is determined by stepping a pinhole at the object plane in and out of focus of the Spectrometer Facility object plane while measuring the blur size at the FPA. The spatial response of the instrument in the cross-track direction was measured in two different ways: with our standard knife-edge MTF measurement procedure and slit PST measurement procedure. A knife-edge target was positioned at the Spectrometer Facility image plane at the end of the light pipe. The edge of the target was perpendicular to the slit of Hyperion. Adjusting the Facility fine pointing mirror to move the knife-edge a fraction of a pixel in the cross-track direction then generates the knife-edge function and producing the results in Figure 5a. Data analysis is then performed in multiple steps. We assume that the instrument transfer function is a convolution of optical blur (assumed to be gaussian) and pixel sampling (top-hat). The point spread function (PSF) is the derivative of the knife-edge data shown in Figure 5b. An alternate to the knife-edge technique is to use a narrow slit to map out the PSF directly. The MTF is the Fourier transform of the PSF and is shown in Figure 5c. Along track MTF is the Fourier transform of the convolution of the PSF in Figure 5b and the along-track smear due to sampling rate and pixel ground footprint considerations. This smearing can be represented as a 'top-hat' function. Thus, the aling-track MTF value at the Nyquist frequency is simply the measured cross-track MTF value multiplied by $2/\pi$.

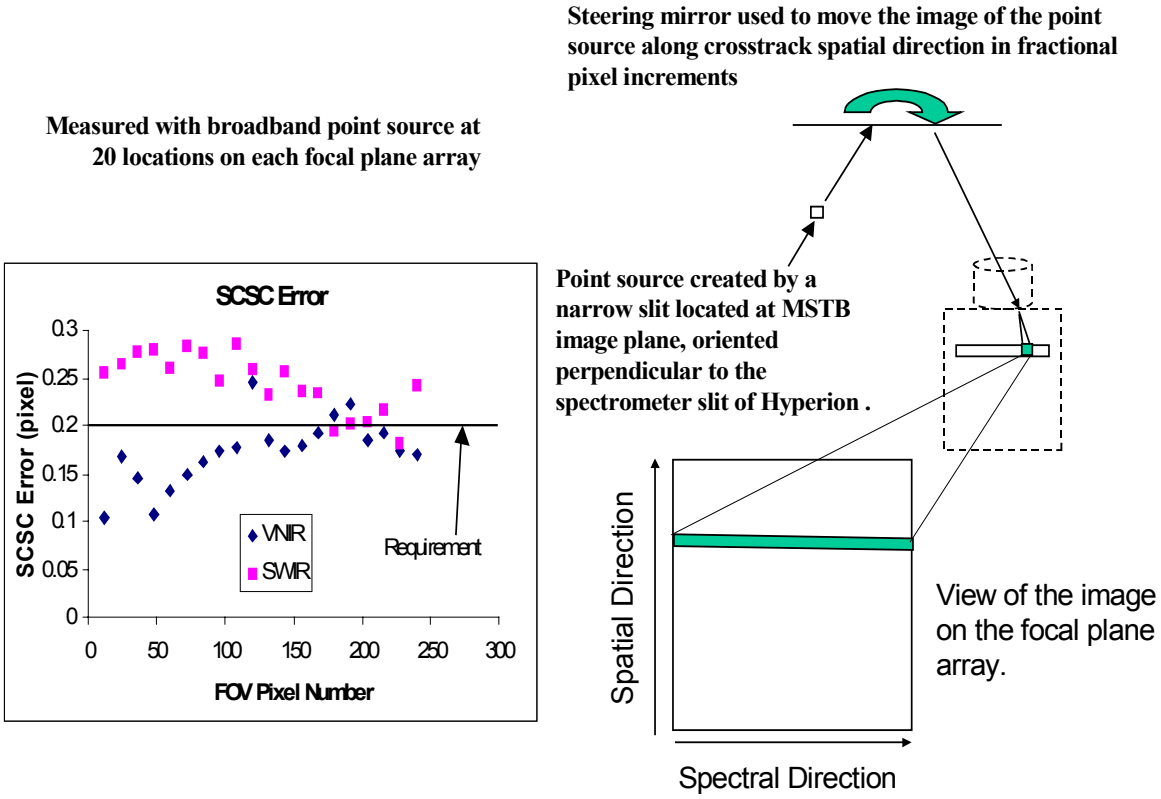

Figure 4 The determination of spatial co-registration of spectral channels.

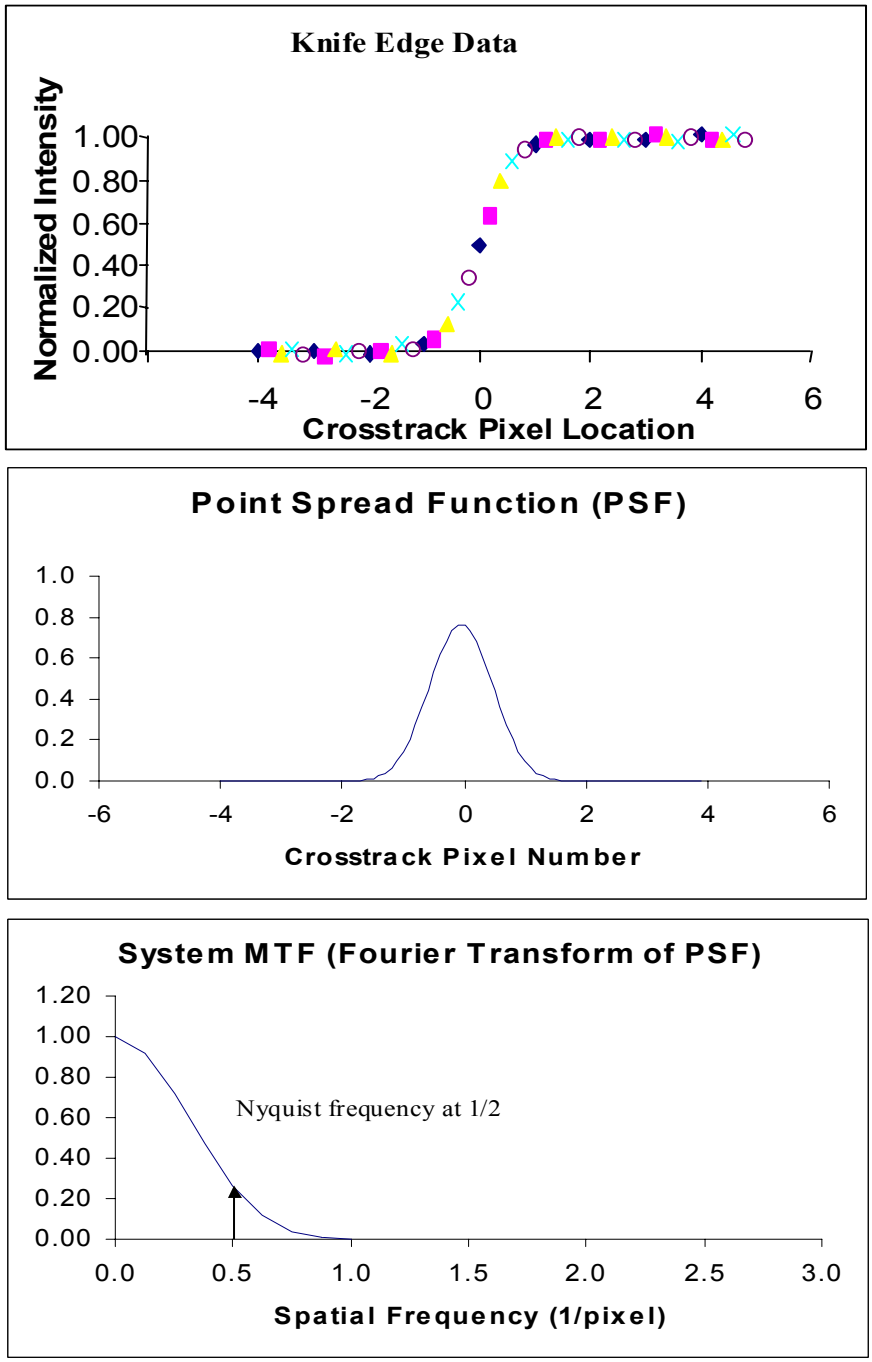

Figure 5 The figures above are a,b, and c in the order of top to bottom

a) Knife Edge Data taken as the Fine Pointing Mirror Motion Uncovers the Pixel
b) Example of a Point Spread Function Derived from (a)
c) Derivation of the MTF from the Fourier Transform of the PSF in (b)

2.3. Hyperion Spectrometer Spectral profile and Spectral Wavelength Calibration

The spectral profile and the center wavelength of each pixel are important for the removal of atmospheric effects because the atmospheric transmittance changes rapidly in wavelength regions of high absorption. The spectral profile is derived using the process for determining CTSA described above. Figure 6 shows examples of the measurement. The curves in the figures are gaussian curves, fitted to the data points. As can be seen from Figure 6, the spectral response function is well approximated by a gaussian with the appropriate width. In addition, we can also deconvolve the effect of light source bandwidth by a similar approach as outlined in the MTF section. The only difference is that instead of using 'knife-edge' step function to represent the light source, we would use the 'tiangular' transmission function of the monochromator. Thus, the spectral response functions can be completely specified by specifying a center channel position and an effective full width at half maximum.

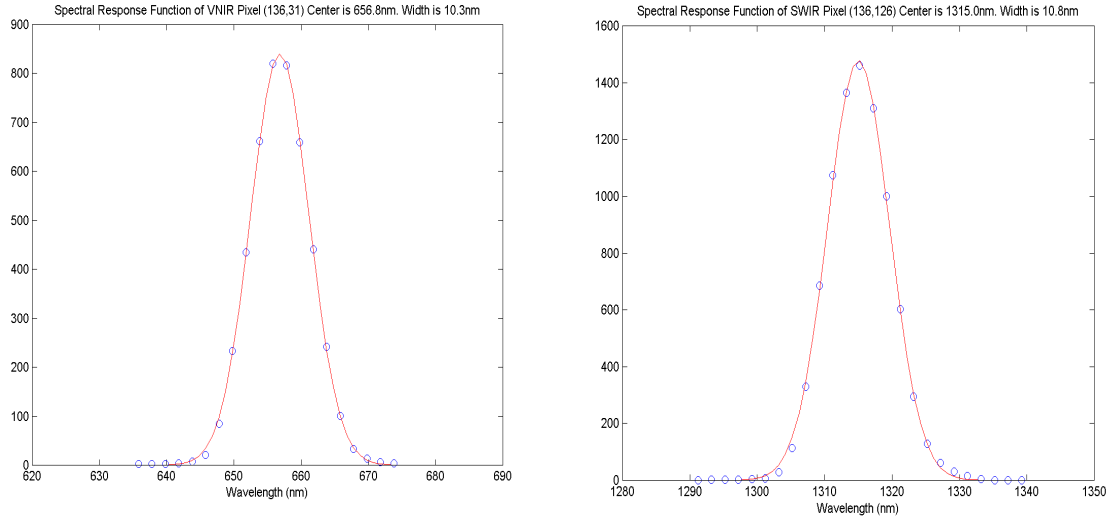

Figure 6 Examples of spectral profile.

There are basically two ways to perform the spectral wavelength calibration. Ideally, one would perform the spectral profile measurement, as described in 2.2.1, for every pixel on the FPA. Since each spectral profile requires 20-25 spectral steps, it would require over $1x10^6$ spectral measurements. Since each spectral measurement takes about 10 seconds to perform, it will require nearly 4000 hours of measurement time. Additional time will also be required for the data analysis. One can quickly see how this is a nearly impossible task! As a compromise, one might measure the spectral profile at selected locations and then perform a 2-dimensional curve fit through the center wavelengths at various FOV's.

Alternatively, one could determine the center wavelengths for every pixel by the doped spectralon technique. Only two frames of data. One is with the FPA flooded with a view of a Spectralon panel with high reflectance at all wavelengths and one with a Spectralon panel doped with a rare earth (holmium oxide and erbium oxide are both used). The ratio of these two images removes the effects of sensor spectral response and lamp spectral output. The wavelength variations of the doped material are well known and stable. By assuming a certain parametric model of the instrument (i.e. its dispersion realitionship and spectral profile) and performing a non-linear least squares fit of the measured ratio to the expected ratio, one can derive the parameters of the underlying model. In addition, the technique can be applied with any source with sharp spectral features. An example of this technique will be on-orbit spectral calibration with atmospheric occultation.

Figure 7 and Figure 8 show the results of the proposed technique. The modeled spectral profile of the FPA is used to convolve with high resolution theoretical curves in Figure 8 (black solid curve) to predict the curve expected for the measured ratio sampled at the Hyperion spectral resolution (blue dotted curve and red solid curve) . The data points are the sensor's normalized response to the two Spectralon panels. The center wavelength values are treated as variables in a non-linear least squares fit of the data points to the curve. This non-linear fit is performed separately

for all 256 spatial points in the FOV. The advantage of using this approach is that all points in the spectrum are used simultaneously to determine the wavelength scale. Further, data for all pixels is collected simultaneously in two frames of data which eliminates the need to collect data laboriously in sub-pixel steps. The regression RMS of the residuals is sensitive to best fit conditions at the 0.05 pixel level. This means that the precision of the technique is good to 5% of a pixel. However, this does not necessarily imply an accuracy of 5%. Accuracy also depend on other factors such as the sufficiency of the model to describe the system and the accuracy of the high resolution theoretical curves. Figure 7 shows the possible accuracy. The blue diamond and red triangle data points were collected at TRW during thermal vaccum testing. As can be seen, the agreement is approximately 0.5 nm (or 5%). The magenta sqaure data points were collected at GSFC after additional vibration testing at the spacecraft level. As can be seen from the data, there appears to be a minor amount of movement of the FPA .

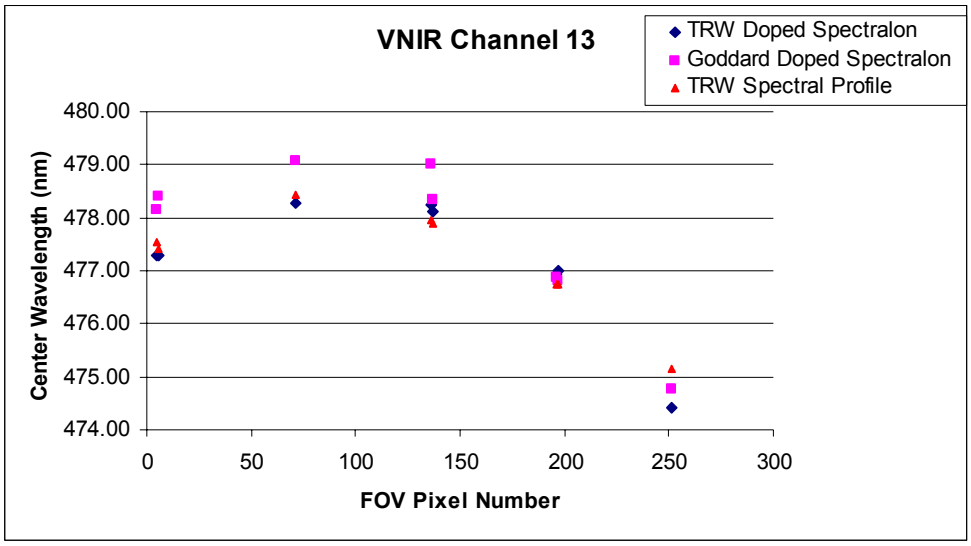

Figure 7 Example of CTSA measurement achieved with different technique

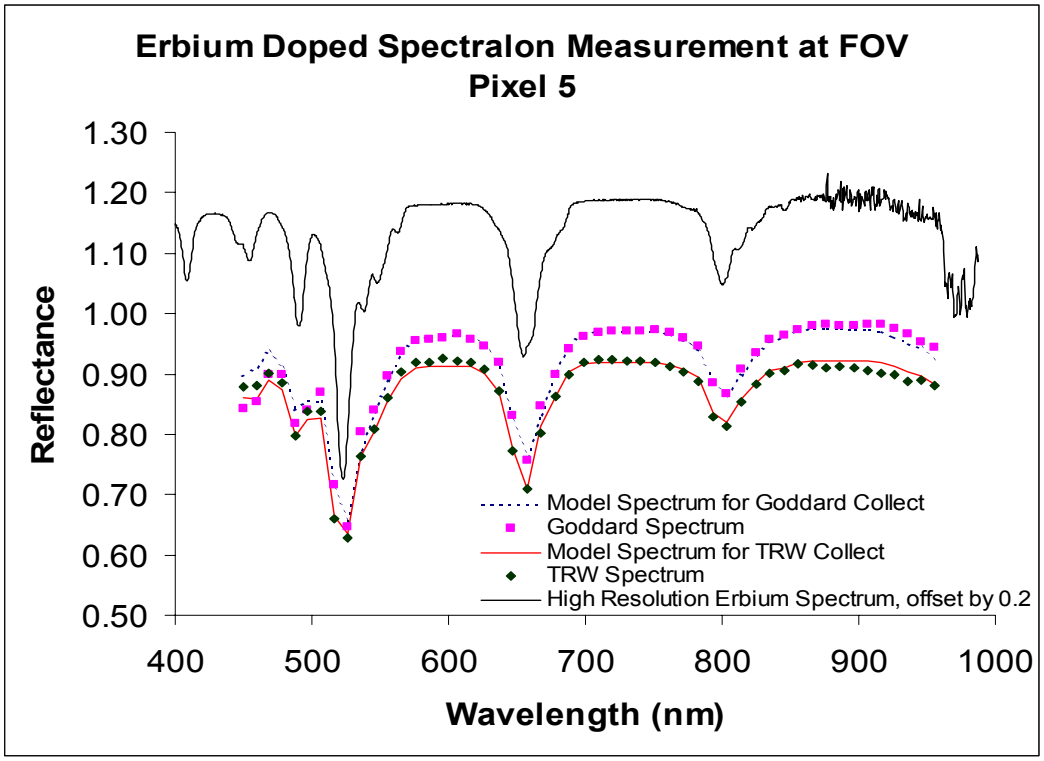

Figure 8 Example of Doped Spectralon curve fit results

2.4. Signal to Noise

Signal to noise ratios were calculated from test data a seven wavelengths using the secondary standard source of radiance the SPA. The Modtran standard model for a zenith angle of 60 degrees and an Albedo of 30 % was calculated and normalized to the data points. The results are shown in Figure 9.

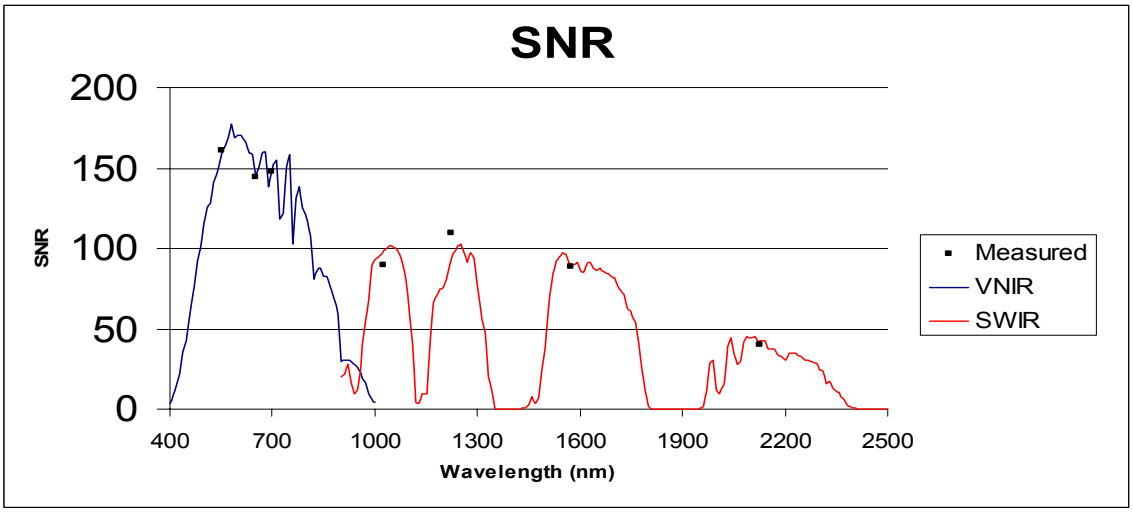

Figure 9 Signal to Noise Results Compared to a Sensor Model Using a Standard Modtran Scene with an Earth Albedo of 30 % and a solar Zenith Angle of 60 degrees. FPA Sensitivity in the Model was Adjusted to Match the Data Points Shown as Black Squares

3. Conclusions

The Hyperion sensor was thoroughly, radiometrically characterized and calibrated with a set of procedures originally developed for characterization of imaging spectrometer instruments at TRW. Upgrades in the Spectrometer Characterization Facility hardware allowed for improved characterization of image quality and spectral wavelength calibration. The doped Spectralon technique allows for center wavelength accuracy that will permit the analysts of imaging spectrometry data to adequately remove atmospheric effects at the edge of rapidly varying atmospheric absorption bands.

Acknowledgements

The authors wish to acknowledge the support of the NASA Goddard Space Flight Center for their support on the Hyperion Program Contract No. NAS5-98161. This work was supported by the Hyperion test team including Glenn Brossus, Pam Clancy, Miguel Figueroa, Mark Frink, John Godden, Darrell Gleichauf, and Momi Ono, and who bore the brunt of the long hours of procedure execution and quick look data validation.

References

1. C. T. Willoughby, J. Marmo, and M. A. Folkman, "Hyperspectral Imaging Payload for the NASA Small Satellite Technology Initiative Program*", IEEE Aerospace applications Conference Proceedings*, IEEE, Aspen, CO, February (1996)
2. M.A. Folkman, R. K. DeLong, C. T. Willoughby, D. A. Gleichauf, S. Thordarson, M. Figueros, W. Procino "TRWIS III: An Aircraft-Based Hyperspctral Imager"*„ :, Proc. Optical Science, Engineering , and Instrumentation Symposium,* **SPIE 2819-15,** (1996).
3. Folkman, Mark A., Gleichauf, D. A., Willoughby, C. T., Thordarson, S., and Quon, B. H., "Performance Characterization and Calibration of the TRWIS III Hyperspectral Imager", *Optical Science, Engineering, and Instrumentation Symposium*, **SPIE vol. 2819-15**, (1996)
4. M. A. Folkman, S. Sandor, S. Thordarson, T. Hedman, D. A. Gleichauf, S. Casement, B. Quon, P. Jarecke, "Updated Rresults from Performance Characterization and Calibration of the TRWIS III Hyperspectral Imager, **SPIE, 3118-17,** 142 (1997).